Author Manuscript

Author Manuscript

Author Manuscript

Author Manuscript

HHS Public Access

Author manuscript

Chem Commun (Camb). Author manuscript; available in PMC 2015 December 15.

Published in final edited form as:

Chem Commun (Camb). 2015 December 15; 52(1): 120–123. doi:10.1039/c5cc08317f.

Croconaine rotaxane for acid activated photothermal heating and ratiometric photoacoustic imaging of acidic pH†

Samit Guha[a], **Gillian Karen Shaw**[a], **Trevor M. Mitcham**[b], **Richard R. Bouchard**[b], and **Bradley D. Smith**[a]

Bradley D. Smith: smith.115@nd.edu

[a]Department of Chemistry and Biochemistry, 236 Nieuwland Science Hall, University of Notre Dame, IN 46556, USA

[b]Department of Imaging Physics, University of Texas MD Anderson Cancer Center, Houston, TX 77054, USA

Abstract

Absorption of 808 nm laser light by liposomes containing a pH sensitive, near-infrared croconaine rotaxane dye increases dramatically in weak acid. A stealth liposome composition permits acid activated, photothermal heating and also acts as an effective nanoparticle probe for ratiometric photoacoustic imaging of acidic pH in deep sample locations, including a living mouse.

Molecules and materials that can absorb near-infrared (NIR) laser light and create localized heating are potentially valuable for numerous therapeutic applications.[1] These photothermal agents can also enhance photoacoustic imaging, an emerging modality in molecular imaging with many performance features that are superior to fluorescence imaging and more amenable to clinical translation.[2] To date, most NIR photothermal agents have absorbance profiles that cannot be chemically modulated. However, many photothermal and photoacoustic applications would be improved if the light absorbing properties could be switched on by specific local conditions. A good example is the tissue acidosis associated with pathological states such as cancer, infection, inflammation, and fibrosis.[3] There are a few reports of NIR agents that can undergo changes in absorbance cross-section due to triggered self-aggregation but an inherent drawback with this approach is a dependence on local concentration which can be hard to control.[4] New NIR absorbing agents are needed with chromophores that can be altered directly by the local chemical environment. A logical strategy is to design appropriate dyes with switchable absorbance, but there are very few NIR chromophores with the correct combination of chemical and photophysical properties.[5] Recently, we discovered that croconaine dyes exhibit excellent laser heating properties.[6] They strongly absorb NIR light ($\varepsilon > 10^5$ M^{-1} cm^{-1}) and have short excited state lifetimes with little fluorescence emission, singlet oxygen generation, or dye photobleaching. We have described a supramolecular encapsulation strategy that modulates a croconaine's NIR absorbance wavelength, but this method is susceptible to the concentration dependence

†Electronic Supplementary Information (ESI) available: Chemical structures, synthesis and characterization; liposome data; photoacoustic Imaging data. See DOI: 10.1039/x0xx00000x

Correspondence to: Bradley D. Smith, smith.115@nd.edu.

Author Manuscript Author Manuscript Author Manuscript Author Manuscript

mentioned above.[6a] Here we report a conceptual advance that is based on the pH dependent croconaine (Croc) dye shown in Figure 1a.[7] The dye's absorption profile can be switched between an anionic basic form (λ_{max} < 660 nm) and a zwitterionic acidic form (λ_{max} <794 nm). An important spectral feature is the relatively narrow bandwidths which permit large amplitude switching of molar absorptivity at the two wavelengths. To utilize the lipophilic Croc dye for biological applications we incorporated it within liposome membranes and employed supramolecular strategies to achieve two crucial photothermal and photoacoustic performance features: stable ratiometric absorption response that is unaltered by laser irradiation, and fine-tuning of the dye p*K*a to match the local pH.

A preliminary study using a 808 nm diode laser showed that irradiation of an ethanol solution of Croc in its basic form created very little sample heating, but conversion to the acidic form greatly enhanced laser induced heating (Figure S1). Formulation of the Croc dye for operation in aqueous solution, was achieved by incorporating it into stealth liposomes as an amphiphilic ion-pair with 1,2-dioleoyl-3-trimethylammonium-propane (DOTAP) as the counter cation.[¶] Stealth liposomes have polyethylene glycol chains protruding from the membrane surface which inhibit liposome aggregation and extend circulation time in the blood stream.[8] Initially, stealth liposomes doped with Croc dye (Croc-SL) were prepared as unilamellar vesicles (diameter = 194 nm) with a composition of POPC:Chol-PEG600:DOTAP:Croc 84:10:3:3 (Figure S3). [¶] The sample color was blue at pH 7.4 due to the Croc conjugate base absorption at 660 nm. Titration with acid abolished the blue color and an intense new peak appeared at 794 nm with a pK_a of 6.5 (Figure 1b, S3). Irradiation of cuvettes containing Croc-SL with an 808 nm diode laser produced acid activated photothermal heating (Figure S3b). Dynamic light scattering measurements indicated that Croc-SL do not change size in acidic pH, but the absorption spectrum slowly broadened with time (Figures 1c and S3, S4). The absorption broadening is consistent with self-aggregation of the zwitterionic Croc conjugate acid within the liposome membrane and is a potential drawback for important applications, such as repetitive photothermal heating and ratiometric photoacoustic imaging of pH (see below). We hypothesized that the problem could be circumvented by trapping the Croc dye within a tetralactam macrocycle and generating an interlocked croconaine rotaxane (CrocRot) (Figure 2a). Even under self-aggregation conditions, we expected the surrounding macrocycle in CrocRot to prevent electronic coupling of the encapsulated dye.[6b] Initial attempts to prepare CrocRot by a direct slippage process in organic solvent or within liposome membranes were unsuccessful, presumably due to the steric bulk of the indolenine dimethyl substituents. Thus, a Leigh-type templated clipping reaction was used to convert Croc dye to CrocRot and the rotaxane structure was elucidated using a battery of spectroscopic methods (Figures S5–S11).[9] As expected, rotaxane formation produced a 22 nm red-shift of the dye absorption maxima.[6] The interlocked CrocRot molecule does not unthread in competitive organic solvents or when it is located within a liposome membrane (Figure S9). We prepared CrocRot doped stealth liposomes (CrocRot-SL) composed of POPC:Chol-PEG600:DOTAP:CrocRot

[¶]Abbreviations: Cholesterol-PEG600 n=10–11 (Ch-PEG600), croconaine (Croc), croconaine rotaxane (CrocRot), 1,2-dioleoyl-3-trimethylammoniumpropane (chloride salt) (DOTAP), *N*-(Carbonyl-methoxypolyethyleneglycol-2000)-1,2-distearoyl-*sn*-glycero-3-phosphoethanolamine (DSPE-PEG2000), Indocyanine Green (ICG), 1-palmitoyl-2-oleoyl-*sn*-glycero-3-phosphocholine (POPC). See Figure S2 for chemical structures.

Author Manuscript Author Manuscript Author Manuscript Author Manuscript

84:10:3:3 (Figure S12)† and found that they exhibited very similar pH dependent changes in absorption spectra as above, with a slightly decreased dye pK_a of <6.0 (Figure 2b and Figure S13). We were pleased to find that the spectral stability of CrocRot-SL was greatly improved; for example, there was very little spectral change after sitting for 24 hours in acidic pH (Figures 2c and S14). As shown in Figure 2d, pH dependent photothermal heating was observed using an 808 diode laser (3.5 W/cm^2), and the high spectral stability of the CrocRot-SL enabled multiple laser heating cycles using the same sample with no measurable change in the absorption profile and photothermal heating response (Figure 2e and Figure S15). CrocRot-SL are highly stable in the presence of serum, biological salts (Figure S16a), and small biomolecules such as glutathione, cysteine, and H_2O_2 (Figure S16b). Furthermore, CrocRot-SL were not toxic to cultured mammalian cells (Figure S16c). These results demonstrate that CrocRot-SL are robust biocompatible nanoparticles that can be switched reversibly between acid and base forms and that they survive strong and repeated laser heating. They likely can be used for photothermal therapy and controlled release in disease states that have tissue acidosis.[10] In addition, they can also be utilized for another important application, namely, ratiometric photoacoustic imaging of acidic pH.

Photothermal agents facilitate photoacoustic imaging by absorbing short-duration, low power density laser pulses (~0.06 W/cm^2) and emitting ultrasound waves which are scattered less than light waves and thus penetrate further through biological media to produce higher resolution images.[2] There is a need for new types of exogenous probes for enhanced photoacoustic imaging. The current literature contains several reports of probes that can be activated by cleavage enzymes to produce changes in signal intensity, but to the best of our knowledge, there is no NIR photoacoustic probe with a rapid ratiometric pH response.[11] A preliminary evaluation of phantoms (narrow tubes oriented parallel to the face of the transducer, see Figure S17) containing ethanol solutions of Croc or CrocRot showed that they generated about the same photoacoustic signal intensities as the commonly used NIR dye indocyanine green (ICG) (Figure S18).[12] We then examined two phantoms containing CrocRot-SL at pH 7.4 or 5.0 and observed that the photoacoustic and absorption spectra at each pH value were closely matched (Figure 3a and S19). Additional photoacoustic imaging studies examined the two phantoms at different depths in a light scattering medium (0.7% milk fat solution) that is opaque to normal fluorescence imaging methods. We found that the difference in phantom pH could easily be distinguished by comparing the ratio of photoacoustic signal intensities at 812 and 690 nm. The image in Figure 3b shows a large difference in ratiometric response (more than 5-fold) for the two phantoms, each located at a depth of 11–13 mm from the transducer face. Additional imaging experiments at phantom depths of 9 and 26 mm confirmed that the photoacoustic signal-to-noise decreased with depth, but the pH dependent 812/690 signal ratio hardly changed.

With these proof-of-concept imaging results in hand we moved to a more demanding biological system to assess the potential of acid sensitive CrocRot-doped liposomes. In some diseases, the tissue pH can be as low as 5.5 (*e.g.*, intracellular endosomes, inflamed tissue)

†Electronic Supplementary Information (ESI) available: Chemical structures, synthesis and characterization; liposome data; photoacoustic Imaging data. See DOI: 10.1039/x0xx00000x

Author Manuscript Author Manuscript Author Manuscript Author Manuscript

but in others it is closer to 6.5 (*e.g.*, extracellular matrix of solid tumors).[3] This means it will be necessary to optimize the pK_a of the CrocRot for each case, to ensure a significant degree of absorbance switching. After examining the literature,[13] we reasoned that the pK_a can be fine-tuned in a rational way by simply adding controlled amounts of appropriately charged amphiphiles to the liposome formulation. To demonstrate the utility of this concept we purposely raised the CrocRot pK_a by substituting the neutral Ch-PEG600 in the CrocRot-SL membrane with anionic DSPE-PEG2000.¶ After a short sequence of trials, we found that a modified liposome formulation composed of POPC:DSPE-PEG2000:DOTAP:CrocRot 79:15:3:3 and given the descriptor name, CrocRot-IVSL, exhibited a pK_a of ~6.5 (Figure 4a and S20). §

To demonstrate the capability of CrocRot-IVSL for *in vivo* photoacoustic imaging we chose to image the pH of peritoneal fluid in a living mouse which is known to be in the range of 6.1–6.3.[14] Following a protocol that was approved by the appropriate animal care and use committee, a single dose of CrocRot-IVSL was injected into the peritoneal cavity of a living mouse (N=2), and the sagittal plane of the mouse abdomen was imaged using co-registered B-mode ultrasound and multi-wavelength photoacoustic imaging. The image in Figure 4b is comprised of a B-mode ultrasound image (grayscale) clearly showing the peritoneal cavity and an overlay (red) depicting the corresponding photoacoustic response when the excitation wavelength was 740 nm. There are three photoacoustic spectra in Figure 4c. One spectrum corresponds to the sample of CrocRot-IVSL in buffer at pH 7.4 before injection into the mouse, and the other two spectra correspond to the different regions-of-interest (ROI) in the mouse peritoneal indicated by the arrows in Figure 4b. A comparison of the two *in vivo* ratiometric photoacoustic scans with the UV/absorption plots indicates a peritoneal pH of 6.0–6.5. ‡ Thus, the *in vivo* imaging correctly identified the weakly acidic pH of the mouse peritoneal. With further development, this photoacoustic method may become a new *in vivo* technique for measuring the pH of peritoneal fluid, which is known to decrease with pathological conditions such as bacterial peritonitis, a frequent complication in patients on peritoneal dialysis.[15] It should also be effective at identifying local regions of weakly acidic tissue associated with other types of disease.[3] In addition, the liposome architecture can be further customized by incorporating drugs or additional imaging reporter groups to make a wide array of novel laser responsive therapeutic and diagnostic agents.[16]

Supplementary Material

Refer to Web version on PubMed Central for supplementary material.

§This result highlights an important technical advantage of pH sensor production by nanoparticle self-assembly versus covalent synthesis of a discrete molecular sensor. Fine-tuning the pK_a of a molecular sensor requires a much longer and more labour intensive cycle of structure redesign and chemical synthesis.

‡Inspection of Figure 4c shows that the two major peaks within the in vivo photoacoustic spectra are slightly red-shifted when compared to the spectrum in buffer before injection. This is attributed to in vivo attenuation of the lower photoacoustic excitation wavelengths by the blood-perfused skin and tissue. This anatomical-dependent variation may explain why the two in vivo photoacoustic spectra from nearby peritoneal locations are slightly different. A goal for future imaging studies is to develop calibration methods that correct these tissue-dependent changes in the in vivo photoacoustic spectrum.

Author Manuscript Author Manuscript Author Manuscript Author Manuscript

Acknowledgments

We are grateful for funding support from the Walther Cancer Foundation Advancing Basic Cancer Research Grant (2013/14) administered by the Harper Cancer Research Institute (USA) and the NIH (GM059078 to B.D.S., and P30 CA016672, S10 OD010403 to R.R.B.).

Notes and references

1. (a) Lal S, Clare SE, Halas NJ. Acc Chem Res. 2008; 41:1842–1851. [PubMed: 19053240] (b) Shanmugam V, Selvakumar S, Yeh CS. Chem Soc Rev. 2014; 43:6254–6287. [PubMed: 24811160] (c) Cheng L, Wang C, Feng L, Yang K, Liu Z. Chem Rev. 2014; 114:10869–10939. [PubMed: 25260098]
2. (a) Zackrisson S, van de Ven SMWY, Gambhir SS. Cancer Res. 2014; 74:979–1004. [PubMed: 24514041] (b) Mallidi S, Luke GP, Emelianov S. Trends Biotechnol. 2011; 29:213–221. [PubMed: 21324541] (c) Wang LV, Hu S. Science. 2012; 335:1458–1462. [PubMed: 22442475]
3. (a) Webb BA, Chimenti M, Jacobson MP, Barber DL. Nat Rev Cancer. 2011; 11:671–677. [PubMed: 21833026] (b) Hashim AI, Zhang X, Wojtkowiakk JW, Gillies RJ. NMR Biomed. 2011; 24:582–591. [PubMed: 21387439] (c) Andreev OA, Dupuy AD, Segala M, Sandugu S, Serra DA, Chichester CO, Engelman DM, Reshetnyak YK. Proc Natl Acad Sci USA. 2007; 104:7893–7898. [PubMed: 17483464] (d) Tsai YT, Zhou J, Weng H, Shen J, Tang L, Hu WJ. Adv Healthcare Mater. 2014; 3:221–229.(e) Okajima F. Cell Signal. 2013; 25:2263–2271. [PubMed: 23917207] (f) Honasoge A, Sontheimer H. Front Physiol. 2013; 4:316. [PubMed: 24198789] (g) Jones KM, Randtke EA, Howison CM, Cardenas-Rodriguez J, Sime PJ, Kottmann MR, Pagel MD. Mol Imaging Biol. 2015; 17:177–184. [PubMed: 25187227]
4. (a) Nam J, Won N, Jin H, Chung H, Kim S. J Am Chem Soc. 2009; 131:13639–13645. [PubMed: 19772360] (b) Nam J, La WG, Hwang S, Ha YS, Park N, Won N, Jung S, Bhang SH, Ma YJ, Cho YM, Jin M, Han J, Shin JY, Wang EK, Kim SG, Cho SH, Yoo J, Kim BS, Kim S. ACS Nano. 2013; 7:3388–3402. [PubMed: 23530622] (c) Dragulescu-Andrasi A, Kothapalli S, Tikhomirov GA, Rao J, Gambhir SS. J Am Chem Soc. 2013; 135:11015–11022. [PubMed: 23859847] (d) Li H, Liu X, Huang N, Ren K, Jin Q, Ji J. ACS Appl Mater Interfaces. 2014; 6:18930–18937. [PubMed: 25286378] (e) Hainfeld JF, O'Connor MJ, Lin P, Qian L, Slatkin DN, Smilowitz HM. PLos One. 2014; 9:e88414. [PubMed: 24520385]
5. Shi W, Ma H. Chem Commun. 2012; 48:8732–8744.
6. Spence GT, Hartland GV, Smith BD. Chem Sci. 2013; 4:4240–4244.Spence GT, Lo SS, Ke C, Destecroix H, Davis AP, Hartland GV, Smith BD. Chem Eur J. 2014; 20:12628–12635. [PubMed: 25146580] For a summary of absorption properties for nanoparticles containing croconaine dyes, see: Devadas MS, Devkota T, Guha S, Shaw SK, Smith BD, Hartland GV. Nanoscale. 2015; 7:9779–9785. [PubMed: 25964049] Guha S, Shaw SK, Spence GT, Roland FM, Smith BD. Langmuir. 2015; 31:7826–7834. [PubMed: 26149326]
7. Encinas C, Otazo E, Rivera L, Miltsov S, Alonso J. Tetrahedron Lett. 2002; 43:8391–8393.
8. Immordino ML, Dosio F, Cattel L. Int J Nanomed. 2006; 1:297–315.
9. Gassensmith JJ, Barr L, Baumes JM, Paek A, Nguyen A, Smith BD. Org Lett. 2008; 10:3343–3346. [PubMed: 18582079]
10. (a) Ju E, Dong K, Liu Z, Pu F, Ren J, Qu X. Adv Funct Mater. 2015; 25:1574–1580.(b) Guo M, Huang J, Deng Y, Shen H, Ma Y, Zhang M, Zhu A, Li Y, Hui H, Wang Y, Yang X, Zhang Z, Chen H. Adv Funct Mater. 2015; 25:59–67.(c) Wu X, Yu M, Lin B, Xing H, Han J, Han S. Chem Sci. 2015; 6:798–803.
11. For examples of photoacoustic probes with chemically or biochemically activated response, see: Pu K, Shuhendler AJ, Jokerst JV, Mei J, Gambhir SS, Bao Z, Rao J. Nat Nanotechnol. 2014; 9:233–239. [PubMed: 24463363] Ray A, Yoon HK, Lee YEK, Kopelman R, Wang X. Analyst. 2013; 138:3126–3130. [PubMed: 23598348] Yang K, Zhu L, Nie L, Sun X, Cheng L, Wu C, Niu G, Chen X, Liu Z. Theranostics. 2014; 4:134–141. [PubMed: 24465271] Levi J, Kothapalli SR, Ma TJ, Hartman K, Khuri-Yakub BT, Gambhir SS. J Am Chem Soc. 2010; 132:11264–11269. [PubMed: 20698693] Razansky D, Harlaar NJ, Hillebrands JL, Taruttis A, Herzog E, Zeebregts CJ, van Dam GM, Ntziachristos V. Mol Imaging Biol. 2012; 14:277–285. [PubMed: 21720908]

Author Manuscript Author Manuscript Author Manuscript Author Manuscript

Cash KJ, Li C, Xia J, Wang LV, Clark HA. ACS Nano. 2015; 9:1692–1698. [PubMed: 25588028] Huang G, Si Z, Yang S, Li C, Xing D. J Mater Chem. 2012; 22:22575–22581.Zhang J, Qiao Z, Yang P, Pan J, Wang L, Wang H. Chin J Chem. 2015; 33:35–52.

12. Beziere N, Lozano N, Nunes A, Salichs J, Queiros D, Kostarelos K, Ntziachristos V. Biomaterials. 2015; 37:415–424. [PubMed: 25453969] For recent insight into the photophysical factors that control photoacoustic signal intensity using dyes, see: Frenette M, Hatamimoslehabadi M, Bellinger-Buckley S, Laoui S, La J, Bag S, Mallidi S, Hasan T, Bouma B, Yelleswarapu C, Rochford J. J Am Chem Soc. 2014; 136:15853–15856. [PubMed: 25329769]
13. (a) Hafez IM, Ansell S, Cullis PR. Biophys J. 2000; 79:1438–1446. [PubMed: 10969005] (b) Shi G, Guo W, Stephenson SM, Lee RJ. J Control Release. 2002; 80:309–319. [PubMed: 11943407]
14. Beck A, Bergner-Rabinowitz S, Ofek I. J Bacteriol. 1969; 100:1204–1207. [PubMed: 4902808]
15. Johno H, Ogata R, Nakajima S, Hiramatsu N, Kobayashi T, Hara H, Kitamura M. Nephrol Dial Transplant. 2012; 27:4053–4060. [PubMed: 22573236]
16. (a) Corato RD, Bealle G, Kolosnjaj-Tabi J, Espinosa A, Clement O, Silva AKA, Menager C, Wilhelm C. ACS Nano. 2015; 9:2904–2916. [PubMed: 25695371] (b) Muthu MS, Leong DT, Mei L, Feng SS. Theranostics. 2014; 4:660–677. [PubMed: 24723986]

Author Manuscript Author Manuscript Author Manuscript Author Manuscript

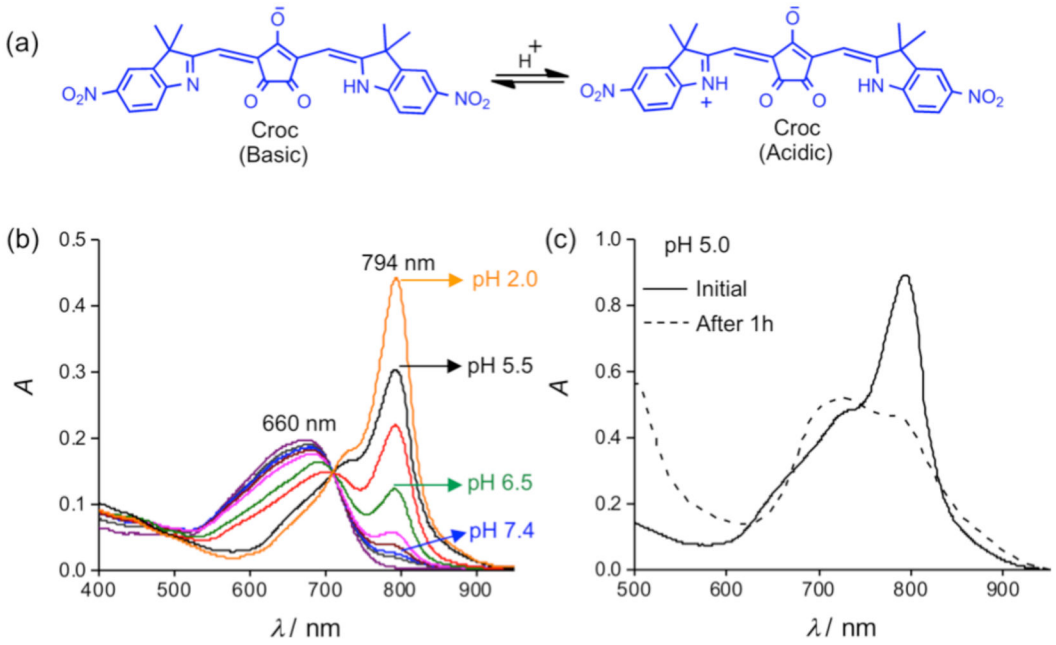

Figure 1.

(a) pH sensitive croconaine (Croc). (b) UV/Vis absorption of Croc-SL in buffer at various pH values, [Croc] = 3 μM. (c) UV/Vis absorption plots of Croc-SL in buffer at pH 5.0, spectra were acquired initially (solid line) and after standing for 1 hour (dashed line) at 4°C.

Author Manuscript Author Manuscript Author Manuscript Author Manuscript

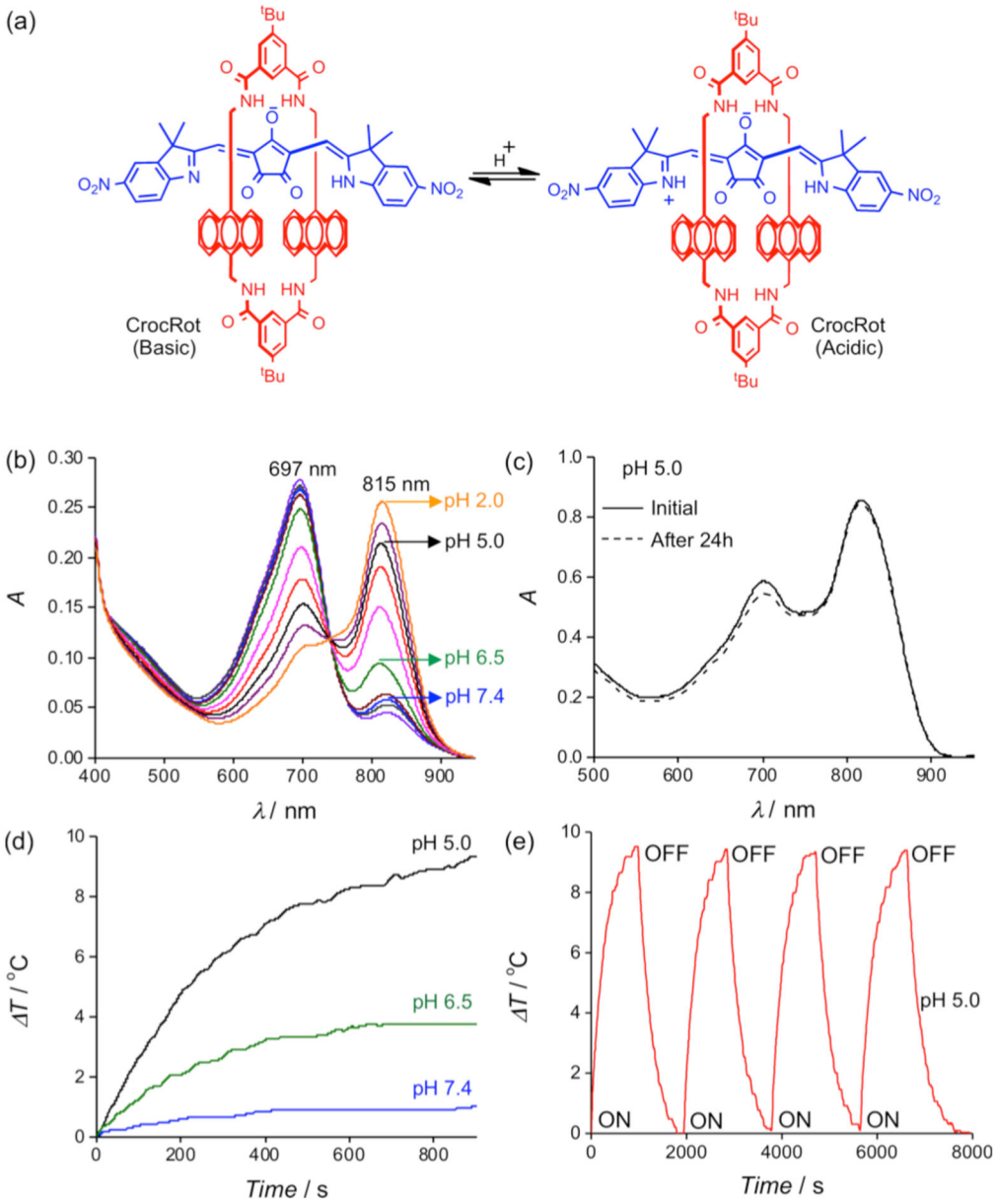

Figure 2.

(a) pH sensitive croconaine rotaxane (CrocRot). (b) UV/Vis absorption of CrocRot-SL at various pH values, [CrocRot] = 3 μM. (c) UV/Vis absorption plots of CrocRot-SL in buffer at pH 5.0, acquired initially (solid line) and after standing for 24 hour (dashed line) at 4°C. (c) Temperature changes during laser irradiation (808 nm, 3.5 W/cm^2) of CrocRot-SL samples at different pH values. (d) Multiple heating cycles of CrocRot-SL at pH 5.0 due to periodic laser irradiation (808 nm).

Author Manuscript Author Manuscript Author Manuscript Author Manuscript

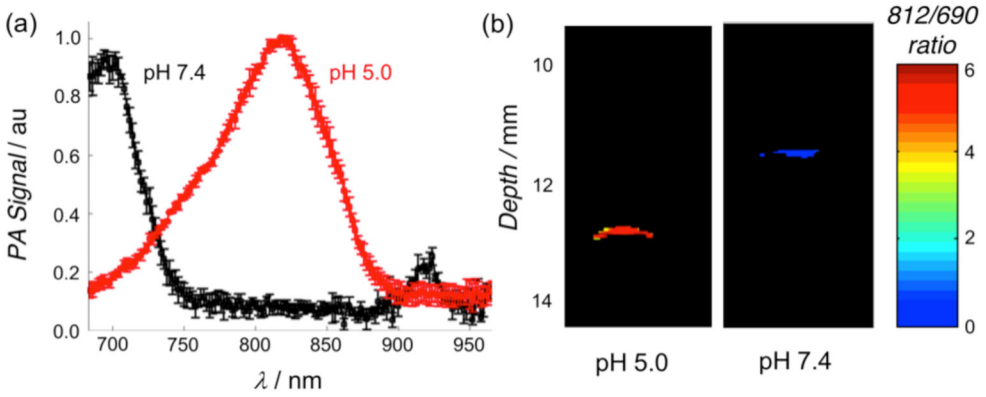

Figure 3.

(a) Photoacoustic scans of CrocRot-SL at pH 7.4 (black) and pH 5.0 (red), mean (N = 3) and SD shown. (b) Ratiometric photoacuostic images of two phantoms containing CrocRot-SL in buffer at pH 7.4 or 5.0, proximally located at 11–13 mm depth in light scattering media. See Figure S17 for a diagram of the transverse orientation of the phantoms.

Author Manuscript Author Manuscript Author Manuscript Author Manuscript

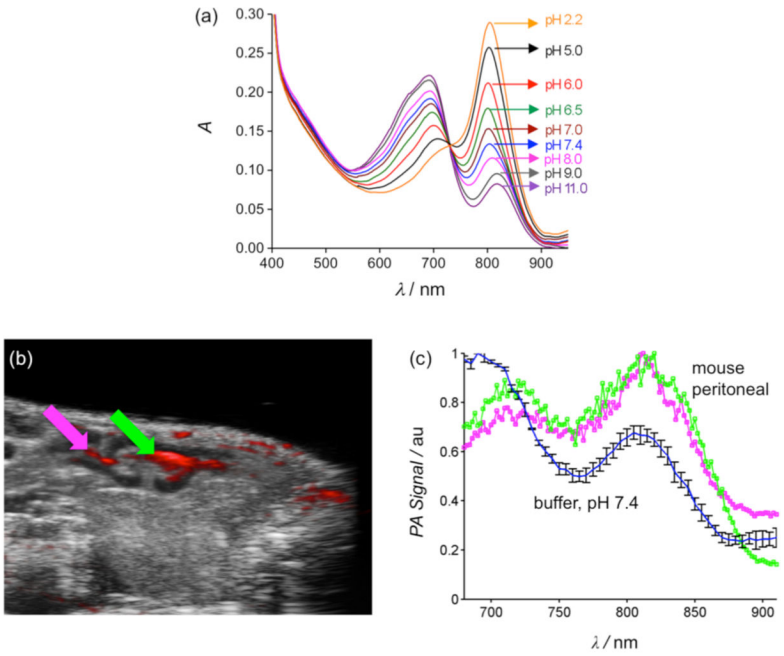

Figure 4.

(a) UV/Vis absorption spectra of CrocRot-IVSL at various pH values, [CrocRot] = 3 μM. (b) Crossectional Bmode ultrasound image (sagittal plane) of living mouse abdomen (grayscale), co-registered with the photoacoustic response at 740 nm; magenta and green arrows denote two ROIs of CrocRot-IVSL accumulation within peritoneal cavity. (c) Photoacoustic spectra of CroRot-IVSL in buffer pH 7.4 before injection (blue/black trace) and in the two ROIs within the mouse peritoneal cavity (magenta and green).